

## Beam-Polarization Observables in $D(\vec{\gamma}, p)n$ and the Nuclear Tensor Force

G. S. Blanpied,<sup>(4)</sup> M. Blecher,<sup>(6)</sup> A. Caracappa,<sup>(1)</sup> C. Djalali,<sup>(4)</sup> M-A. Duval,<sup>(4)</sup> G. Giordano,<sup>(2)</sup> S. Hoblit,<sup>(5)</sup> O. C. Kistner,<sup>(1)</sup> G. Matone,<sup>(2)</sup> L. Miceli,<sup>(1)</sup> W. K. Mize,<sup>(4)</sup> B. M. Preedom,<sup>(4)</sup> A. M. Sandorfi,<sup>(1)</sup> C. Schaerf,<sup>(3)</sup> R. M. Sealock,<sup>(5)</sup> C. E. Thorn,<sup>(1)</sup> S. T. Thornton,<sup>(5)</sup> K. Vaziri,<sup>(7)</sup> and C. S. Whisnant<sup>(1),(4)</sup>

(The LEGS Collaboration)

<sup>(1)</sup>Physics Department, Brookhaven National Laboratory, Upton, New York 11973

<sup>(2)</sup>Istituto Nazionale di Fisica Nucleare, Laboratori Nazionali di Frascati, Frascati, Italy

<sup>(3)</sup>Universita di Roma and Istituto Nazionale di Fisica Nucleare, Sezione di Roma, Rome, Italy

<sup>(4)</sup>Department of Physics, University of South Carolina, Columbia, South Carolina 29208

<sup>(5)</sup>Department of Physics, University of Virginia, Charlottesville, Virginia 22903

<sup>(6)</sup>Physics Department, Virginia Polytechnic Institute and State University, Blacksburg, Virginia 24061

<sup>(7)</sup>Rensselaer Polytechnic Institute, Troy, New York 12180-3590

(Received 29 May 1991)

New precision angular distribution data for the  $D(\vec{\gamma}, p)n$  reaction are presented for incident photon energies of 191 and 222 MeV. The difference of cross sections measured with orthogonal states of linear polarization is sensitive to the short-range behavior of the tensor interaction in models of the nuclear force. Comparisons with the Bonn and Paris potentials illustrate the sensitivity.

PACS numbers: 25.20.-x, 21.30.+y, 24.70.+s, 25.10.+s

The tensor force plays a crucial role in the nucleon-nucleon ( $N$ - $N$ ) interaction. By mixing intrinsic spin and orbital angular momentum, it brings a  $D$ -state component into the deuteron wave function. The tensor interaction comes about largely through one-pion exchange. The low-energy  $D$ -state properties of the two-nucleon system, namely, the quadrupole moment of the deuteron and the asymptotic value for the ratio of the  $D/S$  components in its wave function, are essentially determined by the coupling constant for the  $NN\pi$  vertex which sets the long-range scale of this force. The short-range character of the tensor interaction is undetermined by low-energy deuteron properties, reflecting the fact that deuterium is so loosely bound. However, its short-range behavior has important ramifications when  $N$ - $N$  potentials are used in many-body calculations. This has led to significant uncertainties in modeling the binding energies of few-nucleon systems and the saturation properties of nuclear matter, particularly the binding energy per nucleon and the Fermi momentum [1].

In models of the  $N$ - $N$  interaction, a number of competing effects influence the short-range behavior of the force, for example, vertex form factors, explicit energy dependence in the potentials, and meson-retardation corrections or relativity. Before a  $N$ - $N$  potential can sensibly be used in a many-body calculation, the short-range behavior of the force must be constrained, regardless of how it is apportioned among the different ingredients of the model. We illustrate the sensitivity to the short-range character of the tensor force by comparing calculations using versions of the relativistic one-boson-exchange reduction of the Bonn potential in momentum space (OBEPQ) [1], in which the  $NN\pi$  vertex form factor is adjusted. Here, the

form factor is parametrized as

$$F(q) = \frac{\Lambda^2 - m^2}{\Lambda^2 + q^2},$$

where  $m$  is the pion mass and  $q$  the momentum transfer. The *cutoff mass*  $\Lambda$  governs the effective range of the interaction. Three versions of this model are presented in Ref. [1]. Designated as  $A$ ,  $B$ , and  $C$ , they are obtained by varying  $\Lambda$  (1.3, 1.7, and 3.0 GeV, respectively) while making minimal changes to other parameters of the model.

In phase-shift analyses of  $n$ - $p$  scattering, the amplitudes for  $\Delta l = 2$  orbital angular momentum transitions, particularly the  ${}^3S_1$ - ${}^3D_1$  transition amplitude ( $\varepsilon_1$ ), are sensitive to the short-range behavior of the tensor force. Predictions for  $\varepsilon_1$  from the  $A$ ,  $B$ , and  $C$  versions of the OBEPQ model may be found in Fig. 4.4 of Ref. [1]. Such calculations have been compared to different phase-shift analyses in order to constrain the tensor interaction. However, Chulick *et al.* [2] recently pointed out that, when systematic errors associated with the scattering data are included in the analysis,  $\varepsilon_1$  becomes very poorly determined.

The purpose of this Letter is to identify observables in reaction channels, namely, those associated with the beam polarization in deuteron photodisintegration, which are sensitive to the short-range behavior of the tensor force, and to present definitive data that have the potential of characterizing this behavior.

The photodisintegration of deuterium has a long history with large variations in reported measurements. However, in recent years unpolarized monochromatic photon beams have provided an overdetermination of kinematics

and some convergence in the measured cross sections [3,4]. Experiments with polarized photon beams, produced by coherent bremsstrahlung in diamond crystals [5-7], have reported the asymmetry ( $\Sigma$ ), which is the ratio of the difference to the sum of cross sections obtained with the photon's electric vector parallel and perpendicular to the reaction plane, respectively [ $\Sigma = (d\sigma_{\parallel}/d\Omega - d\sigma_{\perp}/d\Omega)/(d\sigma_{\parallel}/d\Omega + d\sigma_{\perp}/d\Omega)$ ]. This is a difficult technique and the resulting errors in  $\Sigma$  have been appreciable. In addition, the corresponding polarization-independent cross sections have never been measured in the same experiment.

The measurements we report here were performed at the Laser Electron Gamma Source (LEGS) located at the National Synchrotron Light Source of Brookhaven National Laboratory [8]. Linearly polarized  $\gamma$  rays up to 227 MeV in energy were produced by backscattering the 488-nm light of an Ar-ion laser from 2.5 GeV electrons. The energy of the  $\gamma$  rays was determined, to typically 5 MeV, by detecting the scattered electrons in a tagging spectrometer [9]. All of the data in the various energy intervals discussed below were collected simultaneously. Using the polarization of the laser light measured before and after passing through the electron beam, the  $\gamma$ -ray polarization was calculated in a Monte Carlo simulation of the Compton scattering process in the laser-electron interaction region. During the measurements, the polarization was randomly flipped between directions parallel and perpendicular to the reaction plane at a frequency averaging once every 90 sec. The contribution from unpolarized bremsstrahlung in the residual gas of the electron-beam vacuum chamber ( $< 1\%$ ) was also monitored every 90 sec. The net  $\gamma$ -ray polarization ( $-1 \leq P \leq +1$ ) was greater than 0.87 for energies above 185 MeV. The  $\gamma$  flux was monitored by counting  $e^+e^-$  pairs in scintillators interspersed with thin, high- $Z$  converters, and preceded by other detectors which vetoed charged particles. The efficiency of this monitor ( $\sim 4\%$ ) was determined by decreasing the flux and comparing with rates measured in a large NaI(Tl) crystal that was placed directly in the beam. Such measurements were made frequently throughout the experiment.

The target was a liquid-deuterium-filled Mylar cylinder, 3.8 cm in diameter, surrounded by a vacuum chamber with thin Mylar windows. Two different sets of detectors were used to identify protons. One consisted of 21 phoswich assemblies, each a composite of 1-2 mm of  $\text{CaF}_2$  followed by 30-50 cm of plastic scintillator, arranged in groups of three at seven different angles. These assemblies provided energy-loss and total-energy determination. The background contribution ( $\sim 25\%$ ) from reactions within the Mylar of the target walls and of the vacuum chamber window was subtracted in measurements with the target filled with  $^4\text{He}$  gas, normalized to the same integrated photon flux. The  $\gamma$ -ray flux in each energy interval was determined directly from the tagged rate in the  $e^+e^-$  monitors. Data at all angles were col-

lected simultaneously. The second set of proton detectors consisted of four planes of silicon microstrips, providing track reconstruction for each proton, followed by a thin plastic scintillator for energy-loss information and backed by a 25-cm-deep NaI(Tl) for total-energy determination. This detector was positioned opposite to the phoswich array at one of four angles for different periods of the experiment. Its tracking resolution ( $\pm 0.3^\circ$ ) allowed imaging of the source to remove the contributions of the Mylar walls, thus eliminating the need for subtracting empty-target data. For this detector, the  $\gamma$ -ray flux in each energy interval was determined by the Compton scattering Monte Carlo simulation, normalized to the flux in the highest energy tagging interval, as determined by the  $e^+e^-$  monitors. For both sets of detector systems, protons were selected by imposing cuts in energy loss and total-energy deposition. Only tagged photon data were collected with the phoswich array. Here, the kinematics were overdetermined and the proton energy spectrum in each detector was dominated by the two-body  $D(\gamma, p)n$  peak. The microstrip array was operated untagged and the  $\gamma$ -ray energy was reconstructed from the measured proton energy and momentum vector. Comparisons with tagged spectra were used to avoid the kinematic regions contaminated by the  $pp\pi^-$  or  $pn\pi^0$  final states. Corrections for multiple scattering and reactions were calculated with the Monte Carlo code GEANT(3.13) [10]. The results from these two very different sets of instruments agree, and this has greatly aided in the reduction of systematic uncertainties.

The full data set will be described in a forthcoming publication. Here we present only a selection of results that demonstrate the sensitivity of this reaction to the parameters of the  $N$ - $N$  tensor force. The polarization asymmetry is constrained to vanish at  $0^\circ$  and  $180^\circ$  where the azimuthal angle ( $\phi$ ) made by the photon's electric vector with the reaction plane becomes undefined. At low energies the asymmetry approaches  $+1$  at  $90^\circ$  where all models agree. Near pion threshold, interference with the tail of the delta resonance produces a complicated angular pattern and rather small asymmetries. However, near 200 MeV, delta production, which peaks at about 265 MeV in deuterium [3], dominates and produces a simple angular pattern. We suggest that this region can be used to capitalize on the sensitivity to the tensor force.

The polarization-independent cross sections,  $d\sigma/d\Omega = \frac{1}{2}(d\sigma_{\parallel}/d\Omega + d\sigma_{\perp}/d\Omega)$ , and the polarization-difference cross sections,  $\Delta = \frac{1}{2}(d\sigma_{\parallel}/d\Omega - d\sigma_{\perp}/d\Omega)$ , together with their ratio, the asymmetry [ $\Sigma = \Delta/(d\sigma/d\Omega)$ ], are shown as the solid circles in Figs. 1 and 2 for 191- and 222-MeV incident photons, respectively. The indicated errors include the combined statistical and polarization-dependent systematic uncertainties. The vertical bar at  $80^\circ$  in the top and center panels indicates the extent of the polarization-independent systematic errors (5%), those that cancel out of  $\Sigma$ . The polarization-independent cross sections are in very good agreement with the tagged-

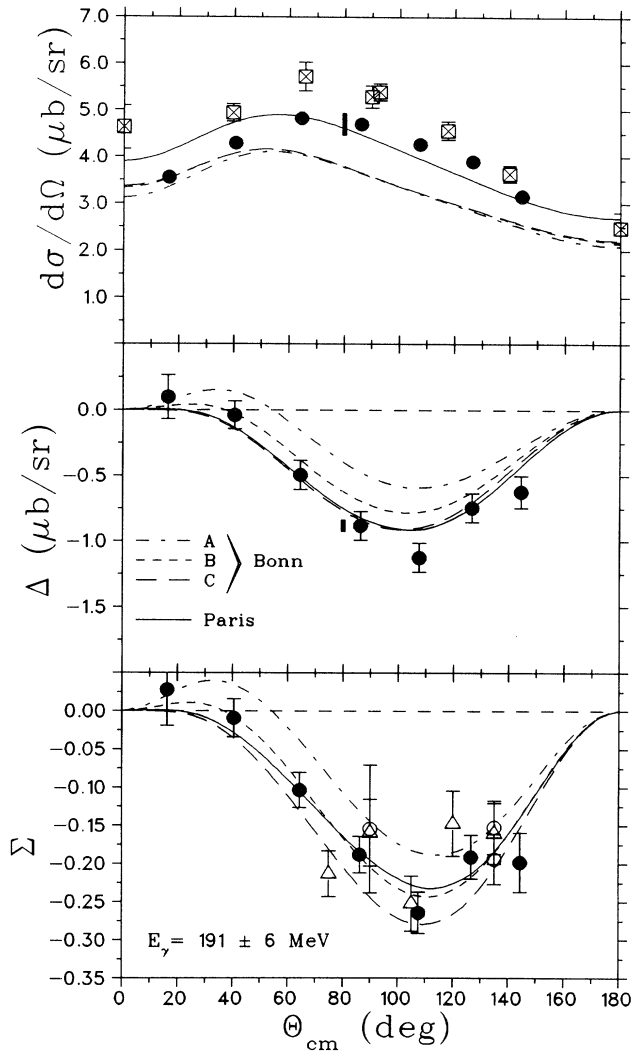


FIG. 1. The  $D(\bar{\gamma},p)n$  polarization-independent  $[d\sigma(\theta)/d\Omega$ , top] and polarization-difference  $[\Delta = \frac{1}{2}(d\sigma_{\parallel}/d\Omega - d\sigma_{\perp}/d\Omega)$ , center] cross sections, at 191 MeV, and their ratio, the asymmetry ( $\Sigma = \Delta/[d\sigma(\theta)/d\Omega]$ , bottom). Solid circles are from this work. The bar at  $80^\circ$  in the top and center panels indicates the 5% polarization-independent systematic error. Open squares with crosses are from Ref. [4], open circles from Ref. [5], and open triangles from Ref. [6]. The curves are from Ref. [11] (Bonn) and Ref. [12] (Paris).

photon data from Bonn [3] at 220 MeV (plotted as the stars in Fig. 2) and at 200 MeV (not shown here). At all energies, the data from Frascati [4] (open squares with crosses) are consistently higher than our results, particularly at forward angles. There are no previously published data on the polarization-difference cross section  $\Delta$ . The published asymmetry data (open symbols) [5–7] have large errors that generally overlap our measurements.

The dashed curves in the figures are from Ref. [11] and

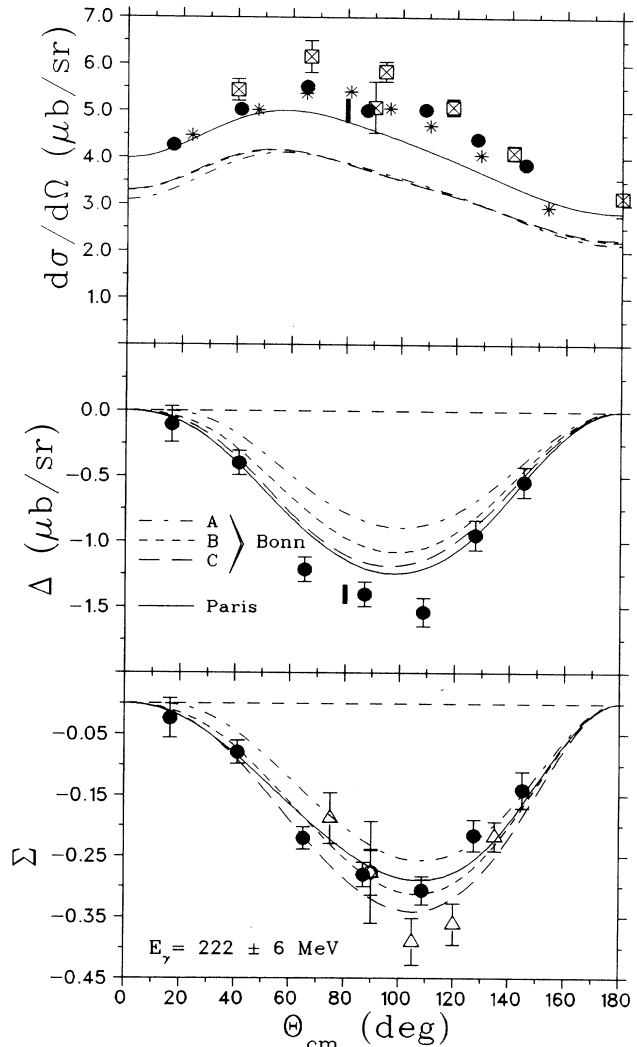


FIG. 2. The  $D(\bar{\gamma},p)n$  observables at 222 MeV. See caption to Fig. 1; stars are from Ref. [3]. An additional datum from Ref. [7] is plotted as the open diamond at  $90^\circ$  in the bottom panel, overlapping a point from Ref. [6].

were calculated with the *A*, *B*, and *C* versions of the Bonn OBEPQ potential. Similar calculations using the Paris potential [12] are also shown (solid lines). In all of these, the reaction dynamics include currents from meson exchange and from the delta isobar, the latter in the impulse approximation, as well as lowest-order relativistic one-body currents and the relativistic spin-orbit current. The calculations using version *B* of the OBEPQ potential are in reasonably good agreement with the asymmetry data. However, the general dependence upon the azimuthal polarization angle  $\phi$  is given by

$$d\sigma(\theta, \phi)/d\Omega = d\sigma(\theta)/d\Omega + P\Delta(\theta)\cos(2\phi),$$

where *P* is the degree of linear polarization. Thus, the in-

dependent observables in the reaction are the polarization-difference ( $\Delta$ ) and polarization-independent cross sections ( $d\sigma/d\Omega$ ). Neither are adequately reproduced by the OBEPQ  $B$  potential and it is merely fortuitous that the discrepancies cancel in their ratio  $\Sigma$ . As evident in both figures, the predictions for  $d\sigma/d\Omega$  using the three different pion cutoff masses in the Bonn OBEPQ potential are indistinguishable. It is  $\Delta$  that exhibits sensitivity to the tensor force. Since the three OBEPQ potential predictions all fall consistently short of measured unpolarized cross sections, there must exist a problem that is not associated with modeling the tensor force. That being the case, it would be premature to adjust the pion cutoff mass in this model to reproduce  $\Delta$ .

The calculations with the Paris potential provide a reasonable representation of the polarization-independent data when systematic errors are taken into account. The most noticeable discrepancy is in the location of the peak in the angular distribution, which these calculations consistently shift to a more forward angle. However, the shape of the predicted angular distribution  $d\sigma(\theta)/d\Omega$  is strongly affected by the relativistic spin-orbit current [13], which contributes significantly at forward and backward angles but has little effect near  $90^\circ$ . Slight errors in this correction can skew  $d\sigma(\theta)/d\Omega$ . However, since the azimuthal polarization angle ( $\phi$ ) becomes undefined at forward and backward angles, the difference cross section  $\Delta(\theta)$  must vanish there, independent of the choice for the  $N$ - $N$  potential. Thus, such corrections have almost no effect on the calculated values for  $\Delta(\theta)$ , and leave outstanding the discrepancies near  $90^\circ$  which become prominent at 222 MeV (Fig. 2, center). One aspect of these calculations remains to be investigated. In all cases, the delta degrees of freedom have been included only in the impulse approximation and the effects of a coupled-channel treatment should be studied. Failing this, the source of the discrepancies in  $\Delta(\theta)$  may lie in the short-range part of the tensor force, which is modeled phenomenologically in the Paris potential and was adjusted to fit values of  $\varepsilon_1$  with unrealistically small errors [2].

In summary, the polarization-difference cross sections

$\Delta(\theta)$  in  $D(\vec{\gamma}, p)n$  exhibit a clear sensitivity to the short-range properties of the tensor interaction. Apparent sensitivities in  $\Sigma$  come solely from  $\Delta$ , the numerator of this asymmetry ratio. The first measurements of  $\Delta$  have been presented here and these have the potential of providing a very useful constraint on the  $N$ - $N$  tensor force.

The LEGS Collaboration is supported by the U.S. Department of Energy under Contracts No. DE-AC02-76-CH00016 and No. DE-FG0589-ER40S0, and in part by the Istituto Nazionale di Fisica Nucleare (Italy) and the U.S. National Science Foundation. W.K.M. is supported by a SURA/CEBAF Fellowship. One of us (A.M.S.) would like to thank H. Arenhoevel and K. M. Schmitt of the University of Mainz for many useful discussions. We also gratefully acknowledge C. Ruth of Rensselaer Polytechnic Institute for cross-checking the GEANT calculations and Dr. D. Dowell for his assistance with the distribution of poisson.

- 
- [1] R. Machleidt, *Adv. Nucl. Phys.* **19**, 189 (1989).
  - [2] G. S. Chulick *et al.*, *Phys. Rev. C* **37**, 1549 (1988).
  - [3] J. Arends *et al.*, *Nucl. Phys.* **A412**, 509 (1984).
  - [4] E. DeSanctis *et al.*, *Phys. Rev. C* **34**, 413 (1986); P. Levi Sandri *et al.*, *Phys. Rev. C* **39**, 1701 (1989).
  - [5] F. F. Liu, *Phys. Rev.* **138**, B1443 (1965).
  - [6] V. G. Gorbenko *et al.*, *Nucl. Phys.* **A381**, 330 (1982).
  - [7] G. Barbiellini *et al.*, *Phys. Rev.* **154**, 988 (1967).
  - [8] A. M. Sandorfi *et al.*, *IEEE Trans. Nucl. Sci.* **30**, 3083 (1983).
  - [9] C. E. Thorn *et al.*, *Nucl. Instrum. Methods Phys. Res., Sect. A* **285**, 447 (1989).
  - [10] R. Brun *et al.*, CERN Report No. CERN DD/EE/84-1, Ver. 3.13, 1987 (unpublished).
  - [11] K. M. Schmitt and H. Arenhoevel (private communication), extensions of *Few Body Syst.* **7**, 95 (1989).
  - [12] P. Wilhelm, W. Leidemann, and H. Arenhoevel (private communication), extensions of calculations in Ref. [13].
  - [13] P. Wilhelm, W. Leidemann, and H. Arenhoevel, *Few Body Syst.* **3**, 111 (1988).